

# A fluorescent AND logic gate driven by electrons and protons

David C. Magri\*

Received (in Montpellier, France) 13th November 2008, Accepted 20th November 2008

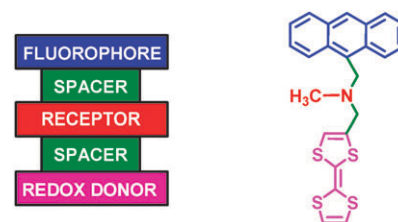
First published as an Advance Article on the web 11th December 2008

DOI: 10.1039/b820313j

**A molecular logic gate displays a fluorescence output after oxidation in acidic media according to AND logic.**

Molecular logic gates responsive to many kinds of chemical and physical inputs, including temperature and light, are known.<sup>1–7</sup> Another physico-chemical property that can be incorporated into molecular logic gates is redox potential.<sup>8</sup> Early examples of redox-fluorescent switches were routinely based on the redox state of a transition metal.<sup>9</sup> Recently, there has been the advancement of a new generation of redox-fluorescent switches founded on the oxidation or reduction of an organic component.<sup>10,11</sup> This has paved the way to the emergence of multi-input molecular logic gates with an electrochemical switching function.<sup>12</sup> One notable example of an AND logic gate responsive to redox and proton stimuli is a two-component molecular-level machine consisting of a macrocyclic polyether and a  $\pi$ -deficient cyclophane as monitored by absorption spectroscopy.<sup>13</sup> Herein is presented a simple AND logic gate **1** that simultaneously processes information regarding the acid concentration and oxidizing ability by communicating a fluorescent light signal.<sup>14,15</sup> Such redox-fluorescent molecules could find application in molecular electronics, and as sensing devices, for example, in monitoring water quality and corrosion in pH-dependent environments. Pourbaix diagrams have long been used to correlate the thermodynamic stability of ionic species as a function of potential and pH.<sup>16</sup>

The characterization and logic operation of **1** is demonstrated in acetonitrile by cyclic voltammetry, constant potential electrolysis, UV-visible absorption and fluorescence spectroscopy. The conceptual design, as illustrated in Scheme 1, is based on a modular photoinduced electron transfer (PET) approach by combining in a single molecule, a proton receptor<sup>1</sup> and a redox-activated switching element<sup>11</sup> according to an unprecedented fluorophore–spacer–receptor–spacer–redox donor format. More specifically, an anthracene fluorophore (blue) is connected to a tertiary amine receptor for  $H^+$ , which is connected to the tetrathiafulvalene (TTF) redox donor (magenta) *via* methylene spacers (green). In its neutral state, **1** is non-emissive because PET from either the unbound receptor or from the redox donor quenches the fluorescence. When the TTF unit is oxidized, in particular to the dication, PET from the redox donor is prevented; however, PET is still possible from the unbound receptor. Similarly, when the



**Scheme 1** Colour-coded conceptual box diagram and molecular structure of the redox-fluorescent AND logic gate **1**.

electron lone pair of the tertiary amine is bound to a proton, PET from the amine is prevented; however, PET from the redox donor is still possible. In either case, little fluorescence is observed. Only when both PET channels are shut 'off', by oxidation of the redox donor and protonation of the receptor, is an enhanced fluorescence observed according to AND logic.

Cyclic voltammetry of **1** in acetonitrile containing 0.10 M tetrabutylammonium perchlorate (TBAP) was examined using a glassy carbon electrode.<sup>17</sup> As shown in Fig. 1a, on scanning to 1.2 V (dashed line), the oxidation of **1** exhibits two reversible redox couples with standard potentials of 0.38 and 0.74 V corresponding to the oxidation of the TTF unit to the radical cation and dication, respectively (see Fig. 1d for comparison). Scanning out to 2.0 V reveals broad, irreversible waves about 1.4 V due to the oxidation of the anthracene and amine moieties. On the return scan, the TTF peak-to-peak widths are no longer consistent with a Nernstian peak separation of 59 mV,<sup>18</sup> suggesting the formation of a redox active product.<sup>19</sup> Repetitive cycling voltammetry between –0.2 and 1.2 V after initially scanning to 2.0 V (Fig. 1b), confirms the presence of four redox couples, the additional two standard potentials at 0.97 and 0.52 V. However, in the presence of 10 mM methanesulfonic acid, the redox couples at 0.97 and 0.52 V are not observed (Fig. 1c). Furthermore, acid causes a positive peak shift of 70 mV in the TTF peaks, and results in the broad waves increasing three-fold in current height with a sharp peak at a potential of 1.29 V. These observations suggest that excess acid prevents a competing reaction pathway from the anthracene radical cation.<sup>19</sup> Voltammograms of authentic TTF and anthracene in Fig. 1d show two reversible redox couples at 0.64 V and 0.27 V for the former and a sharp, irreversible peak potential at 1.5 V for the latter. In 10 mM methanesulfonic acid, no change is observed in the voltammograms of either TTF or anthracene, suggesting that the 70 mV anodic shift in the TTF peaks in Fig. 1c is due to electronic effects from protonation of the tertiary amine.

The UV-visible absorption spectrum in aerated acetonitrile shows both structured and broad tailing absorption bands

Department of Chemistry, 6 University Avenue, Acadia University, Wolfville, Nova Scotia, Canada B4P 2R6.

E-mail: david.magri@acadiau.ca; Fax: (+1) 902 585 1114;

Tel: (+1) 902 585 1468

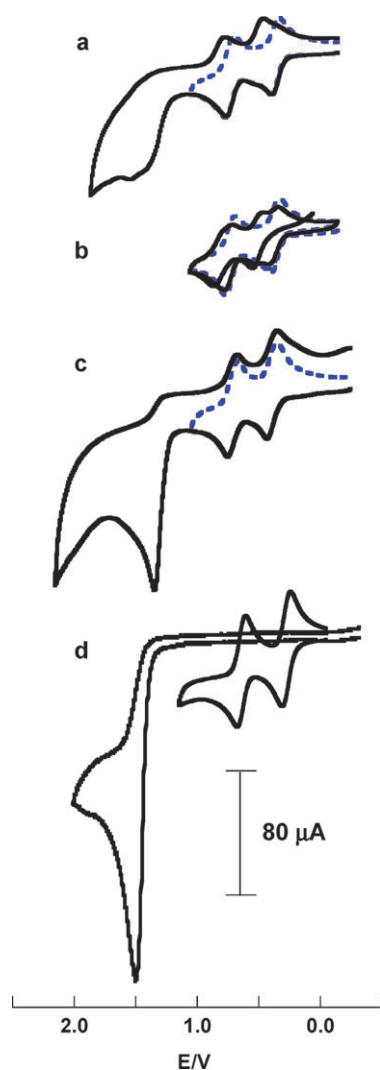


**Fig. 1** (a) Cyclic voltammograms of 1.1 mM **1** in acetonitrile containing 0.10 M TBAP at a glassy carbon electrode at 0.1 V s<sup>-1</sup>. (b) Repetitive cycling voltammetry of 1.1 mM **1**. The dashed line, starting at -0.2 V, corresponds to cycling through the tetrathiafulvalene redox couples between -0.2 and 1.2 V (followed by scanning to a potential of 2.0 V, which has been omitted). The solid line corresponds to switching potentials between -0.2 and 1.2 V. (c) Cyclic voltammograms of 1.0 mM **1** in the presence of 10 mM methanesulfonic acid. (d) Cyclic voltammograms of 1.3 mM anthracene and 1.2 mM tetrathiafulvalene.

(Fig. 2). The well-defined vibrational peaks at 349, 367 and 387 nm with molar extinction coefficients of 7900, 11 000 and 9300 cm<sup>-1</sup> mol<sup>-1</sup> L are characteristic of the anthracene chromophore. The broad band tailing out to 490 nm is attributed to the TTF component. Addition of 50 mM methanesulfonic acid results in the anthracenic peaks red-shifting 4 nm with an isosbestic point at 369 nm (see inset in Fig. 2).

Fig. 2 also illustrates the UV-visible spectra of **1** before and after electrochemical oxidation of the TTF unit with a glassy carbon rotating disk electrode at an applied potential of 0.60 V.<sup>20</sup> Addition of 1 F mol<sup>-1</sup> of charge results in a green-coloured solution and the formation of two new bands centred at 444 nm and 593 nm, which are characteristic of the TTF

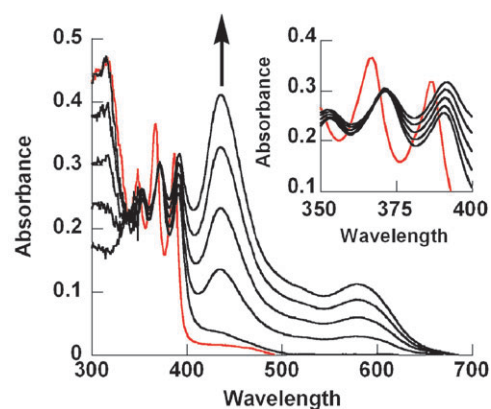


**Fig. 2** UV-visible absorption spectra of  $3 \times 10^{-5}$  M **1** in acetonitrile (red curve). The five black curves are in the presence of 50 mM methanesulfonic acid and increase with 0, 13, 26, 39 and 52 mC (one electron equivalent) of charge added to the solution. The inset highlights the isosbestic point at 369 nm.

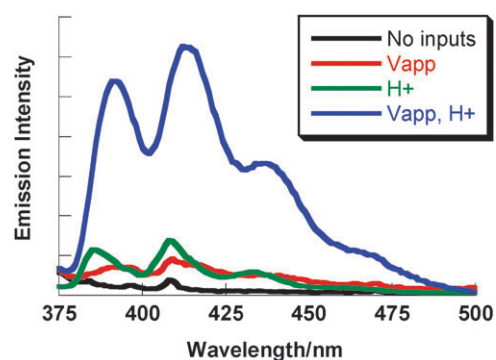


**Fig. 3** Fluorescence spectra of  $10^{-5}$  M **1** in acetonitrile excited at 369 nm. An enhanced fluorescence signal is observed on protonation of the tertiary amine and after oxidation of the TTF redox donor to the dication state.

radical cation.<sup>21</sup> Electrolysis in the presence of 50 mM methanesulfonic acid, as shown in Fig. 2, also yields new bands that are blue-shifted to 435 and 580 nm. Further oxidation to the dication by the addition of another electron equivalent of charge at an applied potential of 0.90 V results in a clear, colourless solution and the disappearance of the radical cation bands.

The digital logic characteristics of **1** in acetonitrile were determined by observing the fluorescence spectra under four experimental conditions. Quantitative details can be found in Fig. 3 and Table 1. In the presence of 10 mM methanesulfonic acid and after two-electron oxidation of the TTF unit, the fluorescence output is significantly high. In the other three logic states the fluorescence output is low, in accordance with AND logic, because of PET from either the unprotonated amine or from the TTF donor to the excited state anthracene.

Addition of one equivalent of Fe(ClO<sub>4</sub>)<sub>3</sub> in place of an applied voltage at an electrode results in similar changes in the absorbance spectrum (Fig. 2).<sup>21</sup> Likewise, a fluorescence enhancement is observed in accordance with AND logic behaviour with one equivalent of Fe(ClO<sub>4</sub>)<sub>3</sub>.<sup>22</sup> However, removal of a second electron by electrochemical oxidation of

**Table 1** Truth table for the AND logic gate **1**<sup>a</sup>

Input <sub>1</sub> (voltage) <sup>b</sup>	Input <sub>2</sub> (H <sup>+</sup> ) <sup>c</sup>	Output emission ( $\phi_F$ ) <sup>d</sup>
0 (low)	0 (low)	0 (low, 0.001)
0 (low)	1 (high)	0 (low, 0.003)
1 (high)	0 (low)	0 (low, 0.002)
1 (high)	1 (high)	1 (high, 0.015) <sup>e</sup>

<sup>a</sup>  $10^{-5}$  M **1** excited at the isosbestic point of 369 nm in acetonitrile.

<sup>b</sup> High input level at an applied voltage of 0.60 V using a 12 mm rotating disk glassy carbon electrode after addition of  $1 \text{ F mol}^{-1}$  of charge. Low input level, no applied voltage. <sup>c</sup> High input level, 10 mM methanesulfonic acid. Low input level, no acid. <sup>d</sup> Relative  $\phi_F$  measured with anthracene in ethanol ( $\phi_F = 0.21$ ).<sup>27</sup> Output level high when  $\phi_F > 0.005$ . <sup>e</sup> Output emission after  $1 \text{ F mol}^{-1}$  of charge or 1 equivalent of  $\text{Fe}(\text{ClO}_4)_3$  is  $\phi_F = 0.009$ . Another  $1 \text{ F mol}^{-1}$  of charge at an applied voltage of 0.90 V yields  $\phi_F = 0.015$ .

the TTF radical cation to the dication at an applied potential of 0.90 V results in a further 50% fluorescence enhancement as shown in Fig 3.

These observations can be rationalized based on thermodynamic calculations. Using the cyclic voltammetry measurements from Fig. 1, the driving force for PET is calculated from the Weller equation.<sup>23</sup> In acetonitrile, PET from the TTF moiety, and from the TTF radical cation, to the excited state anthracene is calculated to be thermodynamically favourable by  $-1.0 \text{ V}$  and  $-0.64 \text{ V}$ , respectively. The fact that the radical cation strongly absorbs at longer wavelengths than the anthracene chromophore (Fig. 2) suggests quenching of the fluorescence may also occur *via* an electronic energy transfer mechanism from the excited anthracene to the TTF radical cation. In contrast, PET from the TTF dication, with a standard potential outside the potential window in Fig. 1, to the excited anthracene is not feasible as the driving force for PET is uphill by at least  $0.6 \text{ V}$ .<sup>23</sup> Also, energy transfer from the excited anthracene to the TTF dication is not possible as the latter does not absorb in the visible spectrum, which is evident from the colourless solution and absorption spectrum (Fig. 2). Hence, the TTF dication is the state from which the fluorescence is switched 'on'.

An interesting outcome from this study is the resulting quantum yield of 0.015 in the 'on' state (Table 1, entry 4), which is an order of magnitude lower in comparison with the anthracene quantum yield of 0.2. This is due to PET from the excited anthracene to the TTF dication to yield anthracene and TTF radical cations. The calculated driving force for this PET reaction is  $-1.2 \text{ V}$ .<sup>24</sup> Such a negative driving force suggests that electron transfer may occur in the Marcus inverted region.<sup>25</sup> This illustrates an uncommon way of limiting the switching factor without completely preventing a fluorescence output. The common limiter of switching factors in PET sensors generally results from the inability of metal cations to sufficiently reduce the HOMO energy of the receptor so that a residual PET in the same direction still competes with fluorescence as observed by a picosecond flash photolysis study.<sup>26</sup> The present case with **1** shows a residual PET in the 'on' state that occurs in the opposite direction to the PET reactions in the 'off' states.

Fluorescence titrations in acetonitrile after oxidation of the TTF to the dication were attempted. A complete titration

curve and evaluation of the proton binding constant were not obtainable due to the difficulty of reliably measuring low concentrations of acid. Nonetheless, a maximum fluorescence emission was observed at an acid concentration of  $3.0 \times 10^{-4} \text{ M}$ . Subsequent addition of up to 50 mM acid did not result in any significant changes in either the fluorescence or UV-visible absorption spectra, which verifies the molecule is stable under acidic, aerobic conditions.

In summary, the redox-fluorescent sensor **1** operates as an AND logic gate by electrochemical (or chemical) oxidation of the TTF moiety and protonation of the tertiary amine. This is a minimal AND logic gate activated by only proton and electron inputs.<sup>13</sup> As **1** is a prototype, a future direction will be towards designing redox-fluorescent logic gates insensitive to fluorescence quenching in the presence of excess transition metal ions. This may lead to a general approach for monitoring the presence of analytes in the environment under varying potential and pH conditions.<sup>16</sup>

The University of Prince Edward Island (UPEI) is acknowledged for a Major Faculty Research Grant. Gratitude is extended to Prof. Brian Wagner (UPEI), and Prof. Mark Workentin and Prof. Robert Hudson at the University of Western Ontario for access to their laboratories and instrumentation. The author thanks Professors A. P. de Silva and Mark Workentin for their insightful discussions and encouragement.

## Experimental

### Instrumentation

The melting point was recorded on a Mel-Temp melting point apparatus. UV-visible absorption and fluorescence spectra were recorded on a Varian Cary 100 UV-visible spectrometer and PTI fluorescence spectrometer, respectively. Infrared spectra were recorded on a Bruker Vector 33 FT-IR spectrometer on NaCl plates. Nuclear magnetic resonance spectra were recorded on a Bruker 300 MHz instrument. <sup>1</sup>H and <sup>13</sup>C NMR spectra were recorded at 300.1 and 75.5 MHz, respectively, with  $\text{CDCl}_3$  as the solvent. Spectra are reported in ppm *vs.* tetramethylsilane ( $\delta = 0.00$ ) for <sup>1</sup>H NMR and  $\text{CDCl}_3$  ( $\delta = 77.00$ ) for <sup>13</sup>C NMR. Mass spectrometry was performed on a MAT 8200 Finnigan high-resolution mass spectrometer by electron impact (EI).

### Electrochemistry

Cyclic voltammetry and constant potential electrolyses were performed using a Perkin-Elmer PAR 263A potentiostat interfaced to a personal computer equipped with PAR 270 electrochemistry software. Experiments were conducted in a water-jacket cell maintained at  $25^\circ\text{C}$  in a copper Faraday cage while purging with a continuous flow of high purity argon to expel oxygen. The working electrode was a 3 mm diameter glassy carbon rod (Tokai, GC-20) sealed in glass tubing. It was activated by first cycling 20 times between 0 and  $-2.8 \text{ V}$  at a scan rate of  $0.2 \text{ V s}^{-1}$  following by cycling 20 times between 0 and  $2.0 \text{ V}$ . The counter electrode was a  $1 \text{ cm}^2$  Pt plate. The reference electrode was a silver wire immersed in a glass tube with a sintered end containing  $0.10 \text{ M}$  tetrabutylammonium

perchlorate (TBAP) in acetonitrile. Internal resistance compensation was applied to minimize the ohmic drop between the working and reference electrode. The reference electrode was calibrated vs. the ferrocene–ferrocenium couple at 0.464 V vs. KCl saturated calomel electrode (SCE) by addition of nitrobenzene (–1.107 V) to the cell after each experiment.

During constant potential electrolyses the working electrode was a 12 mm tipped glassy carbon rotating disk electrode (EDI101) connected to a CTV101 speed control unit from Radiometer Analytical. The counter electrode was a platinum wire immersed in a glass frit. The reference electrode was a silver wire contained in a sintered glass frit and stored in an electrolyte solution before use. The electrolyte solution was pre-electrolysed at a potential several hundred millivolts short of the solvent cutoff. Electrolysis was performed at a constant potential of 0.60 or 0.90 V.

## Synthesis

Compound **1** was synthesized from the precursor 4-formyl-tetrathiafulvalene, which was prepared by reaction of TTF with lithium diisopropylamide and *N*-methylformanilide in THF at –78 °C.<sup>28</sup> Reductive amination of 4-formyltetrathiafulvalene with anthracenemethylamine and sodium triacetoxyborohydride in 1,2-dichloroethane yielded **1**.<sup>29</sup> An orange solid was recovered after purification by flash chromatography on silica gel using a 1 : 1 dichloromethane–hexanes eluant. Overall yield was 10%. Mp 128–130 °C;  $\nu_{\max}(\text{NaCl})/\text{cm}^{-1}$ : 3064, 2944, 2848, 2790, 1338, 1122, 1012, 777, 723;  $\delta_{\text{H}}(300 \text{ MHz}, \text{CDCl}_3, \text{SiMe}_4)$ : 2.30 (s, 3H, NCH<sub>3</sub>), 3.46 (s, 2H, CH<sub>2</sub> spacer<sub>1</sub>), 4.51 (s, 2H, CH<sub>2</sub> spacer<sub>2</sub>), 6.18 (s, 1H, CH), 6.29 (s, 2H, CH), 7.41–7.62 (m, 4H, CH), 7.96–8.06 (d, 2H, *J* = 8.3 Hz, CH), 8.40–8.55 (3H, m, anthracene);  $\delta_{\text{C}}(75.5 \text{ MHz}, \text{CDCl}_3, \text{SiMe}_4)$ : 41.70, 53.32, 57.32, 109.80, 110.69, 114.11, 118.88, 119.12, 124.88, 124.93, 125.76, 127.77, 129.00, 129.26, 131.30, 131.40, 137.06; *m/z*(EI): 439(14), 438(12), 437( $\text{M}^{+}$ , 48), 258(6), 192(18), 191(100), 189(9), 146(10), 86(8), 84(10); calcd for C<sub>23</sub>H<sub>19</sub>NS<sub>4</sub> ( $\text{M}^{+}$ ) 437.0401, found 437.0395.

## References

- Reviews: (a) A. P. de Silva, T. P. Vance, M. E. S. West and G. D. Wright, *Org. Biomol. Chem.*, 2008, **6**, 2468; (b) D. C. Magri, T. P. Vance and A. P. de Silva, *Inorg. Chim. Acta*, 2007, **360**, 751; (c) J. F. Callan, A. P. de Silva and D. C. Magri, *Tetrahedron*, 2005, **61**, 8551; (d) A. P. de Silva and N. D. McClenaghan, *Chem.–Eur. J.*, 2004, **10**, 574.
- Reviews: (a) K. Szacilowski, *Chem. Rev.*, 2008, **108**, 3481; (b) U. Pischel, *Angew. Chem., Int. Ed.*, 2007, **46**, 4026; (c) V. Balzani, A. Credi and M. Venturi, *Chem.–Eur. J.*, 2008, **14**, 26; (d) R. Ballardini, P. Ceroni, A. Credi, M. T. Gandolfi, M. Maestri, M. Semarano, M. Venturi and V. Balzani, *Adv. Funct. Mater.*, 2007, **17**, 740; (e) A. Credi, *Angew. Chem., Int. Ed.*, 2007, **46**, 5472; (f) D. Gust, T. A. Moore and A. L. Moore, *Chem. Commun.*, 2006, 1169; (g) V. Balzani, A. Credi and M. Venturi, *ChemPhysChem*, 2003, **4**, 49.
- Examples of logic gates based on light and heat inputs: (a) S. D. Straight, P. A. Liddell, Y. Terazono, T. A. Moore, A. L. Moore and D. Gust, *Adv. Funct. Mater.*, 2007, **17**, 777; (b) J. Andréasson, S. D. Straight, G. Kodis, C.-D. Park, M. Hambourger, M. Gervald, B. Albinsson, T. A. Moore, A. L. Moore and D. Gust, *J. Am. Chem. Soc.*, 2006, **128**, 16259; (c) S. D. Straight, J. Andréasson, G. Kodis, S. Bandyopadhyay, R. H. Mitchell, T. A. Moore, A. L. Moore and D. Gust, *J. Am. Chem. Soc.*, 2005, **127**, 9403; (d) G. Y. Jiang, Y. L. Song, X. F. Guo, D. Q. Zhang and D. B. Zhu, *Adv. Mater. (Weinheim, Ger.)*, 2008, **20**, 2888; (e) X. F. Guo, D. Q. Zhang and D. B. Zhu, *Adv. Mater. (Weinheim, Ger.)*, 2004, **16**, 125; (f) M. Irie, *Chem. Rev.*, 2000, **100**, 1685; (g) K. Szacilowski, *Chem.–Eur. J.*, 2004, **10**, 2520; (h) M. Tomasulo and F. M. Raymo, *Chem.–Eur. J.*, 2006, **12**, 3186; (i) F. M. Raymo, *Adv. Mater. (Weinheim, Ger.)*, 2002, **14**, 401; (j) S. Uchiyama, N. Kawai, A. P. de Silva and K. Iwai, *J. Am. Chem. Soc.*, 2004, **126**, 3032; (k) F. Remacle, R. Weinkauf and R. D. Levine, *J. Phys. Chem. A*, 2006, **110**, 177.
- (a) D. Margulies, C. E. Felder, G. Melman and A. Shanzer, *J. Am. Chem. Soc.*, 2007, **129**, 347; (b) D. Margulies, G. Melman and A. Shanzer, *J. Am. Chem. Soc.*, 2006, **128**, 4865; (c) D. Margulies, G. Melman and A. Shanzer, *Nat. Mater.*, 2005, **4**, 768; (d) D. Margulies, G. Melman, C. E. Felder, R. Arad-Yellin and A. Shanzer, *J. Am. Chem. Soc.*, 2004, **126**, 15400.
- Examples of logic gates based on chemical inputs: (a) M. Kluciar, R. Ferreira, B. de Castro and U. Pischel, *J. Org. Chem.*, 2008, **73**, 6079; (b) U. Pischel and B. Heller, *New J. Chem.*, 2008, **32**, 395; (c) J. H. Qian, X. H. Qian, Y. F. Xu and S. Y. Zhang, *Chem. Commun.*, 2008, 4141; (d) K. Rurack, C. Trieflinger, A. Kovalchuck and J. Daub, *Chem.–Eur. J.*, 2007, **13**, 8998; (e) A. P. de Silva, M. P. James, B. O. F. McKinney, D. A. Pears and S. M. Weir, *Nat. Mater.*, 2006, **5**, 787; (f) D. H. Qu, Q. C. Wang and H. Tian, *Angew. Chem., Int. Ed.*, 2005, **44**, 5296; (g) A. Coskun, E. Deniz and E. U. Akkaya, *Org. Lett.*, 2005, **5**, 1587; (h) J.-M. Montenegro, E. Perez-Inestrosa, D. Collado, Y. Vida and R. Suau, *Org. Lett.*, 2004, **6**, 2353; (i) S. Langford and T. Yann, *J. Am. Chem. Soc.*, 2003, **125**, 11198 (*J. Am. Chem. Soc.*, 2003, **125**, 14951).
- Examples of logic gates based on enzymes: (a) G. Strack, M. Ornatska, M. Pita and E. Kratz, *J. Am. Chem. Soc.*, 2008, **130**, 4234; (b) R. Baron, O. Lioubashevski, E. Kratz, T. Niazov and I. Willner, *Angew. Chem., Int. Ed.*, 2006, **45**, 1572; (c) R. Baron, O. Lioubashevski, E. Kratz, T. Niazov and I. Willner, *J. Phys. Chem. A*, 2006, **110**, 8548; (d) T. Niazov, R. Baron, E. Kratz, O. Lioubashevski and I. Willner, *Proc. Natl. Acad. Sci. U. S. A.*, 2006, **103**, 17160.
- Examples of logic gates based on DNA oligonucleotides: (a) H. Lederman, J. Macdonald, D. Stefanovic and M. N. Stojanovic, *Biochemistry*, 2006, **45**, 1194; (b) M. N. Stojanovic and D. Stefanovic, *Nat. Biotechnol.*, 2003, **21**, 1069; (c) M. N. Stojanovic and D. Stefanovic, *J. Am. Chem. Soc.*, 2003, **125**, 6673; (d) M. N. Stojanovic, T. E. Mitchell and D. Stefanovic, *J. Am. Chem. Soc.*, 2002, **124**, 3555.
- (a) *Molecular Switches*, ed. B. L. Feringa, Wiley-VCH, Weinheim, Germany, 2001; (b) M. R. Bryce, *J. Mater. Chem.*, 2000, **10**, 589.
- (a) V. Amendola, L. Fabbrizzi, F. Foti, M. Licchelli, C. Mangano, P. Pallavicini, A. Poggi, D. Sacchi and A. Taglietti, *Coord. Chem. Rev.*, 2006, **250**, 273; (b) L. Fabbrizzi, M. Licchelli and P. Pallavicini, *Acc. Chem. Res.*, 1999, **32**, 846; (c) S. Arounaguir and B. G. Maiya, *Inorg. Chem.*, 1999, **38**, 842; (d) V. Goulle, A. Harriman and J.-M. Lehn, *J. Chem. Soc., Chem. Commun.*, 1993, 1034.
- Recent examples of redox-fluorescent switches: (a) R. L. Zhang, Z. L. Wang, Y. S. Wu, H. B. Fu and J. N. Yao, *Org. Lett.*, 2008, **10**, 3065; (b) A. C. Benniston, G. Copley, K. J. Elliott, R. W. Harrington and W. Clegg, *Eur. J. Org. Chem.*, 2008, 2705; (c) R. Martínez, I. Ratera, A. Tàrraga, P. Molina and J. Veciana, *Chem. Commun.*, 2006, 3809; (d) X. W. Xiao, W. Xu, D. Q. Zhang, H. Xu, L. Liu and D. B. Zhu, *New J. Chem.*, 2005, **29**, 1291; (e) S. Leroy-Lhez, J. Baffreau, L. Perrin, E. Levillain, M. Allain, M.-J. Blesa and P. Hudhomme, *J. Org. Chem.*, 2005, **70**, 6313; (f) H. Li, J. O. Jeppesen, E. Levillain and J. Becher, *Chem. Commun.*, 2003, 846.
- G. X. Zhang, D. Q. Zhang, X. F. Guo and D. B. Zhu, *Org. Lett.*, 2004, **6**, 1209.
- (a) C. J. Fang, Z. Zhu, W. Sun, C. H. Xu and C. H. Yan, *New J. Chem.*, 2007, **31**, 580; (b) M. Biancardo, C. Bignozzi, H. Doyle and G. Redmond, *Chem. Commun.*, 2005, 3918; (c) T. Komura, G. Y. Niu, T. Yamaguchi and M. Asano, *Electrochim. Acta*, 2003, **48**, 631.

- 13 P. R. Ashton, V. Baldoni, V. Balzani, A. Credi, H. D. A. Hoffmann, M.-V. Martínez-Díaz, F. M. Raymo, J. F. Stoddart and M. Venturi, *Chem.–Eur. J.*, 2001, **7**, 3482.
- 14 Examples of AND logic gates with ion inputs: (a) D. C. Magri, G. J. Brown, G. D. McClean and A. P. de Silva, *J. Am. Chem. Soc.*, 2006, **128**, 4950; (b) D. C. Magri, G. D. Coen, R. L. Boyd and A. P. de Silva, *Anal. Chim. Acta*, 2006, **568**, 156; (c) S. Uchiyama, G. D. McClean, K. Iwai and A. P. de Silva, *J. Am. Chem. Soc.*, 2005, **127**, 8920; (d) A. P. de Silva, H. Q. N. Gunaratne and C. P. McCoy, *J. Am. Chem. Soc.*, 1997, **119**, 7891; (e) A. P. de Silva, H. Q. N. Gunaratne and C. P. McCoy, *Nature*, 1993, **364**, 42.
- 15 Other examples of AND logic gates with ion inputs: (a) B. Bag and P. K. Bharadwaj, *Chem. Commun.*, 2005, 513; (b) S. J. M. Koskela, T. M. Fyles and T. D. James, *Chem. Commun.*, 2005, 945; (c) H. M. Wang, D. Q. Zhang, X. F. Guo, L. Y. Zhu, Z. G. Shuai and D. B. Zhu, *Chem. Commun.*, 2004, 670; (d) C. R. Cooper and T. D. James, *Chem. Commun.*, 1997, 1419.
- 16 M. Pourbaix, *Atlas of Electrochemical Equilibria in Aqueous Solutions*, Pergamon Press, Oxford, 1966.
- 17 D. C. Magri and M. S. Workentin, *Chem.–Eur. J.*, 2008, **14**, 1698. Potentials are referenced vs. SCE.
- 18 A. J. Bard and L. R. Faulkner, *Electrochemical Methods Fundamentals and Applications*, Wiley, Toronto, 2001.
- 19 V. D. Parker, *Acc. Chem. Res.*, 1984, **17**, 243. Substituted anthracene radical cations are known to dimerize and to act as strong acids. The redox active product may be resulting from some reactivity associated with the tertiary amine for the additional redox couples are not observed at elevated proton concentrations.
- 20 The coulometric titrations are based on Faraday's Law  $q = nmF$  where  $q$  is the charge consumption,  $n$  is the number of electrons,  $m$  is the number of moles and  $F$  is Faraday's constant  $96\,485\text{ C mol}^{-1}$ .
- 21 (a) Y. C. Zhou, H. Wu, L. Qu, D. Q. Zhang and D. B. Zhu, *J. Phys. Chem. B*, 2006, **110**, 15676; (b) A. Credi, M. Montalti, V. Balzani, S. J. Langford, F. M. Raymo and J. F. Stoddart, *New J. Chem.*, 1998, **22**, 1061.
- 22 As reported for an anthracene–TTF–anthracene triad (ref. 11), a second equivalent of ferric ion was found to quench the anthracene fluorescence.
- 23 A. Weller, *Pure Appl. Chem.*, 1968, **16**, 115. The driving force for PET is calculated from  $\Delta G_{\text{PET}} = E_{\text{OX}} - E_{\text{RED}} - E_{\text{S}} - e^2/\epsilon r$  where  $E_{\text{OX}}$  is either the oxidation potential of TTF (0.38 eV), or TTF radical cation (0.74 eV) or TTF dication ( $\geq 2.0$  eV),  $E_{\text{RED}}$  is the reduction potential of anthracene (–1.9 eV),  $E_{\text{S}}$  is the singlet excited energy of anthracene (3.20 eV) and  $e^2/\epsilon r$  is the coulombic term to account for electrostatic interactions (0.10 eV).
- 24 Calculated using  $E_{\text{OX}}$  of anthracene (1.4 eV) and  $E_{\text{RED}}$  of TTF dication (–0.74 eV). Refer to ref. 23.
- 25 R. A. Marcus and N. Sutin, *Biochim. Biophys. Acta*, 1985, **811**, 265.
- 26 H. Kawai, T. Nagamura, T. Mori and K. Yoshida, *J. Phys. Chem. A*, 1999, **103**, 660.
- 27 S. L. Murov, I. Carmichael and G. L. Hug, *Handbook of Photochemistry*, Marcel Dekker Inc., New York, 1993.
- 28 J. Garin, J. Orduna, S. Uriel, A. J. Moore, M. R. Bryce, S. Wegener, D. S. Yufit and J. A. K. Howard, *Synthesis*, 1994, 489.
- 29 A. F. Abdel-Magid, K. G. Carson, B. D. Harris, C. A. Maryanoff and R. D. Shah, *J. Org. Chem.*, 1996, **61**, 3849.